

Journal of Composite Materials

<http://jcm.sagepub.com/>

Polyamide-6-based composites reinforced with pristine or functionalized multi-walled carbon nanotubes produced using melt extrusion technique

Nasir Mahmood, Mohammad Islam, Asad Hameed, Shaukat Saeed and Ahmad Nawaz Khan

Journal of Composite Materials 2014 48: 1197 originally published online 18 April 2013

DOI: 10.1177/0021998313484779

The online version of this article can be found at:

<http://jcm.sagepub.com/content/48/10/1197>

Published by:



<http://www.sagepublications.com>

On behalf of:



[American Society for Composites](#)

Additional services and information for *Journal of Composite Materials* can be found at:

Email Alerts: <http://jcm.sagepub.com/cgi/alerts>

Subscriptions: <http://jcm.sagepub.com/subscriptions>

Reprints: <http://www.sagepub.com/journalsReprints.nav>

Permissions: <http://www.sagepub.com/journalsPermissions.nav>

Citations: <http://jcm.sagepub.com/content/48/10/1197.refs.html>

>> [Version of Record](#) - Apr 16, 2014

[OnlineFirst Version of Record](#) - Apr 18, 2013

[What is This?](#)

Polyamide-6-based composites reinforced with pristine or functionalized multi-walled carbon nanotubes produced using melt extrusion technique

Nasir Mahmood¹, Mohammad Islam^{2,3}, Asad Hameed²,
Shaukat Saeed⁴ and Ahmad Nawaz Khan²

Abstract

Polyamide-6-based composites with pristine or functionalized multi-walled carbon nanotubes were produced using melt extrusion technique. After chemical functionalization, defect formation and attachment of carboxylic ($-\text{COOH}$) or amine ($-\text{NH}_2$) groups on carbon nanotubes was confirmed from high-resolution transmission electron microscope and Fourier transform infra-red spectroscopy studies. Carbon nanotubes incorporation promoted growth of α -form crystals with enhanced thermal stability through increase in crystallization temperature from 162 to 192°C. Dynamic mechanical thermal analysis (DMTA) indirectly pointed out to a homogeneous, uniform dispersion of nanotubes with reduction in free volume of the polymer, exhibiting a slight increase in glass transition temperature and a significant drop in coefficient of thermal expansion value. Composites containing 0.5 wt% NH_2 -carbon nanotubes show increases in elastic modulus and tensile strength by ~ 60 and 76%, respectively. Uniform dispersion and high interfacial strength was manifested by drop in strain to failure and lack of evidence of carbon nanotubes debonding from the matrix.

Keywords

Carbon nanotubes, nanocomposites, polyamide 6, melt extrusion, mechanical properties

Introduction

Multi-walled carbon nanotubes (MWCNT) can be considered as coaxial cylinders of rolled graphene sheets, with inter-cylinder spacing in the range of 0.342 to 0.375 nm¹ depending on the diameter, and lengths of up to several millimeters. Beside outstanding electrical, optical, thermal, and magnetic properties, these nanotubes also offer exceptional mechanical properties as manifested by measured values of Young's modulus and tensile strength to be 1.2 TPa and 50–200 GPa, respectively.² Thus, MWCNT being one-dimensional structures with high-aspect ratio have strong potential both as a replacement of conventional fibers and as an added nanofiller along with woven or laminated fibers,³ in polymer-based composites with resulting advantages of similar or better mechanical properties through much less degree of nanotubes loading. MWCNT use as reinforcement in a polymer matrix can lead to development of composites that are easy to process, flexible, chemically inert, and have low weight. Since CNTs

have extremely high surface area, they tend to agglomerate due to weak van der Waals forces. Also, the hydrophobic nature of nanotubes results in poor interface formation between MWCNT and the polymer. Thus, in order to ensure a homogeneous, agglomeration-free dispersion within the polymeric matrix and to have reasonable interfacial strength, the surfaces of

¹Department of Advanced Materials and Nanotechnology, College of Engineering, Peking University, Beijing, PR China

²School of Chemical and Materials Engineering (SCME), National University of Sciences and Technology (NUST), Islamabad, Pakistan

³Center of Excellence for Research in Engineering Materials (CEREM), Advanced Manufacturing Institute, King Saud University, Riyadh, Saudi Arabia

⁴Department of Metallurgy and Materials Engineering, Pakistan Institute of Engineering and Applied Sciences (PIEAS), Islamabad, Pakistan

Corresponding author:

Mohammad Islam, Center of Excellence for Research in Engineering Materials (CEREM), Advanced Manufacturing Institute, King Saud University, P.O. Box 800, Riyadh 11421, Saudi Arabia.
Email: miqureshi@ksu.edu.sa

nanotubes must be modified. Based on the nature of CNT/polymer interaction, there are four strategies for nanotube mixing or dispersion namely; covalent linkage, non-covalent blending or mixing, specific adsorption or assembly, and compounding of previously functionalized CNT.⁴ Whereas approaches involving physical adsorption such as van der Waals forces and/or π - π stacking are not damaging to the nanotubes and facilitate re-dispersion, they result in weak CNT interaction with the polymer, while the converse is true for chemical and defect functionalization routes.⁵

Among several thermoplastic polymers, polyamide commonly known as nylon is the most versatile polymer offering more strong interactions with nanotubes than other polymers. Polyamide-6 (PA6, polycaprolactam) is one of the most widely used materials in engineering products and is therefore being aggressively explored for reinforcement with different types of nanotubes.^{6–10} Primarily, efforts have focused on pristine or purified MWCNT incorporation with melt processing route found to yield better results,^{7,11} presumably due to application of intense shear forces during blending of nanotubes with the polymer melt that enhances dispersion as well as induces some degree of alignment among nanotubes. Yu et al.¹² reported an increase of $\sim 27\%$ in thermal conductivity and an increase in glass transition temperature by 10°C upon 2.1 wt% pristine MWCNT addition into PA6, with an associated increase in crystallinity. Another study reported a three-fold increase in the values of modulus of elasticity and tensile strength through aligned MWCNT use and stretching of the resulting CNT/Nylon 6,6 composites.¹³

In this paper, we report fabrication of CNT/PA6 composites through incorporation of pristine or functionalized nanotubes with relatively low loading. Using melt extrusion technique, composites with certain loading levels of pristine or functionalized (with carboxylic acid $-\text{COOH}$ or amine $-\text{NH}_2$ groups) were produced and investigated for structural, compositional, thermal, and mechanical properties. The modification of tensile properties including modulus of elasticity, tensile strength, and strain to failure with respect to neat PA6 are described and discussed.

Experimental

All the chemical reagents used for purification and attachment of functional groups such as hydrochloric acid (HCl), nitric acid (HNO_3), sulfuric acid (H_2SO_4), tetrahydrofuran ($\text{C}_4\text{H}_8\text{O}$), thionyl chloride (SOCl_2), and ethylenediamine ($\text{C}_2\text{H}_4(\text{NH}_2)_2$) were of analytical grade with purity level of $>99.99\%$. MWCNT were purchased from Sun Nanotech Company, China, and used either in as-received form or after functionalization. Commercially available PA6 was procured from

local market and was used without any further pretreatment.

CNT functionalization

A total of 3 g MWCNT were refluxed with HCl at 80°C for 6 h and filtered followed by addition into HNO_3 and H_2SO_4 mixed solution (1:3 v/v ratio). After ultrasonic vibration for 2 h and magnetic stirring at 50°C for 1 h, the reflux reaction was carried out at 85°C for 12 h. The MWCNT/acid mixture was washed with distilled water for several times till a pH of ~ 7 was obtained. The filtrate containing COOH -functionalized MWCNT was dried in oven at 110°C for 12 h. Heat treatment at 350°C for 30 min was performed to ensure removal of any traces of acids. After grinding of the dried material for 15 min, a black powder was obtained; 0.7 g of this powder was added in 250 mL of SOCl_2 and sonicated for 1 h. Substitution of $-\text{COOH}$ by $-\text{OCl}$ group was ensured through reflux process at 60°C for 24 h. After SOCl_2 evaporation, any traces of excess SOCl_2 were removed using $\text{C}_4\text{H}_8\text{O}$ (40 mL), followed by vacuum drying at 50°C for 1 h. To produce NH_2 -functionalized CNT, 1 g of dry powder was dispersed in $\text{C}_2\text{H}_4(\text{NH}_2)_2$ and mixed ultrasonically for 6 h. The refluxing treatment at 85°C for 48 h led to attachment of amine group to the nanotubes. Ethylenediamine was evaporated at 80°C under vacuum and the resulting black residue was thoroughly washed in ethanol. Oven drying at 100°C for 2 h was carried out to extract amine-functionalized (N-CNT) nanotubes. Throughout this paper, pristine, carboxylic-, and amine functionalized MWCNT are referred to as P-CNT, C-CNT, and N-CNT, respectively.

Melt processing of CNT/PA6 composites

As opposed to solution mixing technique, melt extrusion process for fabricating composites does not result in voids in the final product. In our case, minilab HAAKE Twin Extruder Mixer (Thermo scientific) was used for making composites with different CNT loadings. The process involved mixing 10 g of commercially available PA6, in granular form, with 0.5 or 1.0 wt% of P-CNT, C-CNT, or N-CNT nanotubes at 250°C temperature and a screw speed of 40 r/min. To ensure homogeneous dispersion and a significant degree of alignment, the procedure was repeated 6 times for each sample. The fibers so obtained were used for various analytical studies. Using HAAKE MiniJet Piston Injection Molding System (Thermo scientific), moulds were made for tensile testing. The samples were heated to 250°C and subsequently injected into the mould at 250 bar pressure. For dynamic mechanical analysis (DMA) studies, 0.3-mm

thick sheets were formed using hot press at 230°C and 400 bar pressure.

Characterization

P-CNT and the fractured surfaces of various CNT/PA6 composites were examined under scanning electron microscope (SEM) (JEOL JSM 6460) and high-resolution transmission electron microscope (HRTEM) (Hitachi HNAR9000). The phase analysis was performed using X-ray diffraction (XRD) (STOE Stadi MP), while the melting point and the crystallization temperature were measured using differential scanning calorimeter (DSC) (Mettler Toledo DSC 823e) under nitrogen flow. The information regarding attachment of various functional groups to the nanotube surface and the chemical nature of composites surfaces was retrieved from attenuation-total-reflection, Fourier transform infra-red spectroscopy (ATR-FTIR) (JASCO FTIR-4100). Thermal analysis of the composites was carried out by operating thermogravimetric analyzer (TG/DTA) (TA Instruments Pyris 1 diamond Q5000IR) at a rate of 10°C/min in nitrogen atmosphere.

Mechanical testing

In accordance with ASTM D-638 standard Type I, all the dogbone specimens for tensile testing had a gage length of 20 mm. The ASTM standard followed is technically equivalent to ISO 527-1. The tests were carried out on a universal testing machine (TINIUS OLSEN 4465) at room temperature and cross-head speed of 5 mm/min. For each sample composition, at least three tests were conducted and the values of Young's modulus, tensile strength, and percent elongation were averaged.

DMA studies were carried out on TMA (Perkin Elmer, Q400), a machine that is capable of performing both DMA and thermomechanical analysis (TMA). The specimens were in the shape of thin sheets with approximate dimensions of 20 × 3 × 0.3 mm. During the tests, the specimens were heated from room temperature to ~220°C at heating rate and frequency of 3°C/min and 1 Hz, respectively.

Results and discussion

Structural, chemical, and compositional characterization

The SEM image of the P-CNT is shown in Figure 1(a). The CNT diameter was found to be in the range of ~30 to 40 nm with an average diameter of ~34 nm. The length of the nanotubes was measured to be of

the order of few microns. Low and high magnification HRTEM images of an individual nanotube are presented in Figure 1(b), (c). It is evident that strong oxidizing agents (H₂SO₄ and HNO₃) produce oxygenated sites as defects on the sidewalls of the CNTs. The discontinuity in the outermost shells and slight detachment from inner shells, as evident in Figure 1(c), is indicative of defects generated on the outer surface due to ultrasonication treatment.⁵ This finding is also supported by Raman spectra (not shown here) that exhibited an increase in the intensity of D band representative of disordered sp³ carbon on CNT. The absence of catalyst nanoparticles during TEM examination confirmed their removal during initial treatment with HCl. Comparison of FTIR spectra for pristine and functionalized CNT (not shown here) also confirmed attachment of desired functional groups.

The chemical nature of the neat PA6 and CNT/PA6 composites was explored using FTIR studies. Due to small loading level of nanotubes into polyamide matrix and the similarities in chemical composition of the matrix and the nanotubes, however, the signature spectra do not significantly differ. The characteristic FTIR spectra for neat PA6 and 0.5 N-CNT/PA6 composite samples are shown in Figure 2. The major absorption band located at 3298 cm⁻¹ can be attributed to N-H stretching mode vibrations from nylon matrix. The presence of two main bands at 2931 and 2860 cm⁻¹ is due to asymmetric and symmetric stretching vibrations of H-C-H groups. The absorption band at 1635 cm⁻¹ represents amide I (C=O stretching vibrations), whereas stretching frequency observed at 1540 cm⁻¹ corresponds to amide II (a combination of N-H bending vibration and stretching vibration of the C-N bond) and/or CH₂ asymmetric deformation. In addition to these bands, the respective positions and the chemical moieties responsible for appearance of several other bands are described as follows: 3084 cm⁻¹ (C-H asymmetric stretching); 1462 cm⁻¹ (C=C atomic stretching); 1431 cm⁻¹ (N-H deformation/CH₂ scissoring); 1264 cm⁻¹ (-S=O); 1171 cm⁻¹ (C-C-H symmetric bending/CH₂ twisting); 1110 cm⁻¹ (C-C-H symmetric bending); 1082 cm⁻¹ (-OH); 1052 cm⁻¹ (C-O, -OH); 730 cm⁻¹ (N-H wagging/CH₂ rocking); 630 cm⁻¹ (C-C bending); 583 cm⁻¹ (O=C-N bending).¹⁴⁻¹⁷

XRD studies of the neat PA6 sample revealed presence of a main peak and two surrounding shoulder peaks, as shown in Figure 3. The strong peak centered at 21.28° represents γ form crystals, whereas the other two peaks are characteristic of α form. The diffraction peaks representative of α form crystals indicate reflections from (200) and (002, 022) planes corresponding to 2θ values of 20.48° and 23.24°, respectively. It is, therefore, concluded that neat PA6 composed of a mixture

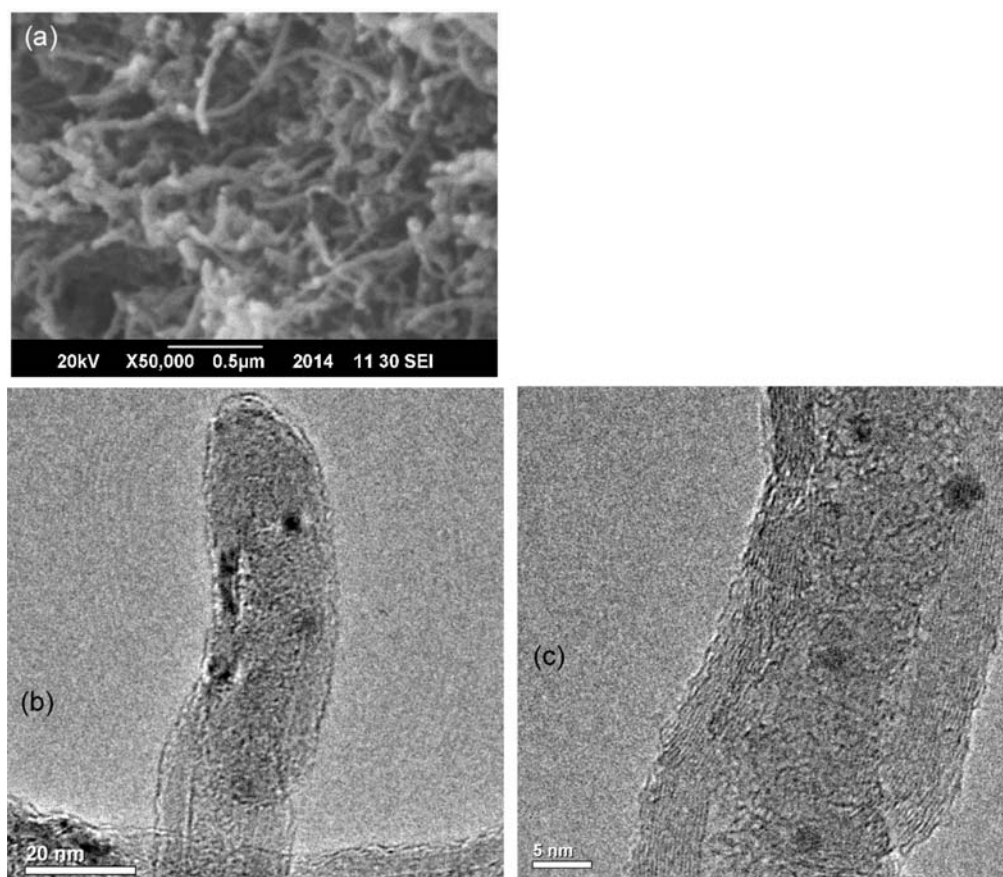


Figure 1. (a) SEM microstructure of the as-received MWCNT and (b), (c) low and high magnification HRTEM images of a MWCNT after $-\text{COOH}$ group functionalization.

SEM: scanning electron microscope; MWCNT: multi-walled carbon nanotubes; HRTEM: high-resolution transmission electron microscope.

of α and γ crystalline forms with γ being the principal phase. It is noteworthy that α is the thermodynamically stable phase consisting of sheets of hydrogen-bonded chains that are packed in an anti-parallel fashion, whereas the γ -phase is the least stable phase formed as a result of random hydrogen bonding between parallel chains.¹¹ The incorporation of CNTs, whether pristine or functionalized, in small amount was found to influence the crystalline nature of PA6 in such manner that the peaks characteristic of the α form crystals became more intense, diminishing the peak indicative of γ form crystals. Thus, the composites were found to be predominantly composed of α phase crystals. The degree of crystallinity was noticed to increase upon increasing the CNT content from 0.5 to 1.0 wt%. Also, in case of functionalized CNT, the reflection from (002, 220) was greater in intensity than that from (200) plane. Thus, MWCNT presence enhances degree of crystallinity and stability of the resulting composites through formation of α form crystals by providing nucleation sites for end-tethering of α form crystals. No diffraction peaks characteristic of MWCNT were

seen in the spectra obtained. Using Sherrer equation ($t = 0.94 \lambda / \beta \cos \theta$), the crystallite size (t) corresponding to α_{200} , α_{002} , 220, and γ_{002} diffraction peaks was determined for all the samples, as listed in Table 1. The value of t was noticed to increase from ~ 2.2 to 7.8 nm upon CNT addition, indicating enhancement of degree of crystallinity due to CNT incorporation. Similar behavior was reported in case of nylon 66/MWCNT composites.¹⁸

Thermal properties

Thermal stability of the neat as well as PA6 composite samples with different MWCNT types and loadings was assessed for a temperature range of ambient to 600°C. No drastic reduction in weight was observed for temperatures up to $\sim 400^\circ\text{C}$, although composites containing P-CNT exhibited greater thermal stability. As shown in Figure 4, the thermogram of the 0.5 P-CNT/PA6 composite indicates that the onset of decomposition occurs at a higher temperature than that for other compositions, implying greater degree of

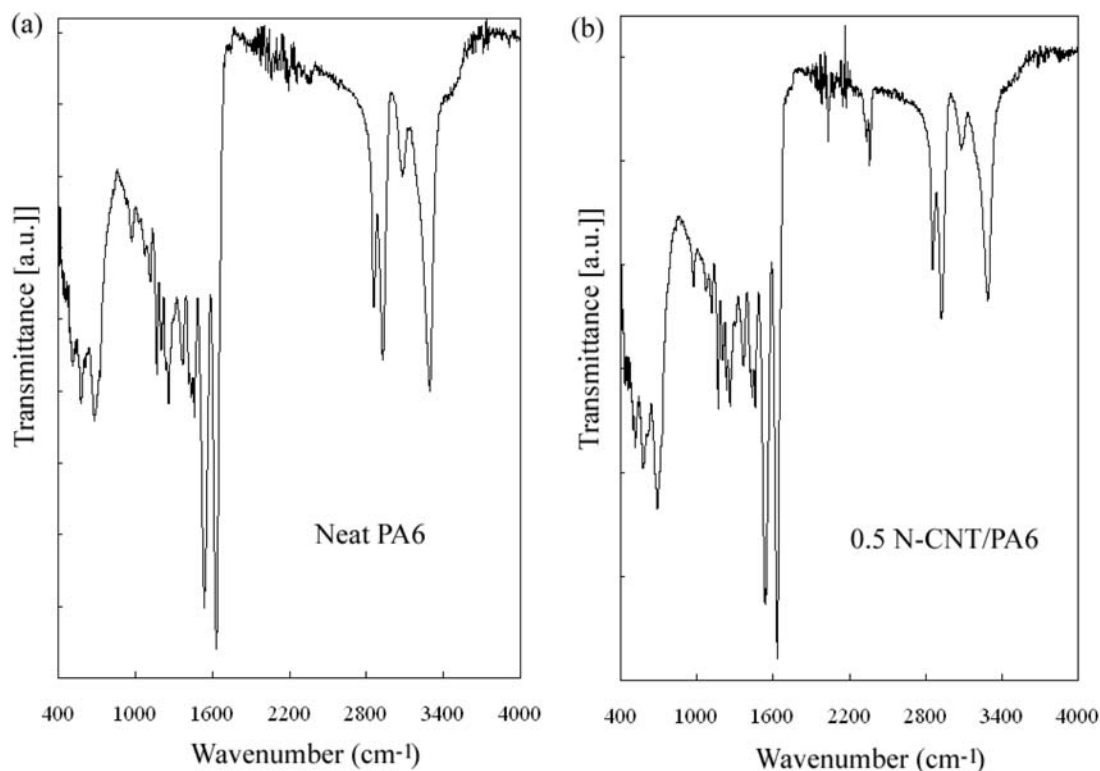


Figure 2. FTIR spectra of neat PA6 and 0.5 N-CNT/PA6 composite samples. FTIR: Fourier transform infra-red spectroscopy; PA6: polyamide-6.

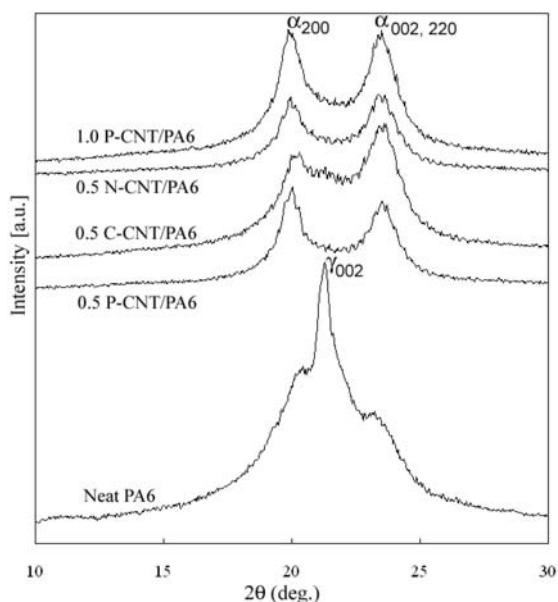


Figure 3. X-ray diffraction spectra of neat PA6 and various CNT/PA6 composites. CNT: carbon nanotubes; PA6: polyamide-6.

thermodynamic stability. Whereas incorporation of P-CNT by 0.5 wt% into PA6 matrix delayed thermal degradation by up to 10°C, addition of 0.5 wt% N-CNT caused slight deterioration in thermal

properties of the resulting composite as compared to neat PA6. Thus, addition of P-CNT leads to an improvement in thermal properties through enhanced degree of crystallization and preferential formation of α form crystals. Further increase in loading of P-CNT to 1.0 wt% results in similar or slightly better thermal attributes, probably due to difficulties in uniform dispersion of nanotubes in the PA6 matrix. Since functionalization of the nanotubes introduces defects on the sidewalls of the nanotubes and reduces their length as well,¹⁹ deterioration in thermal stability compared to neat PA6 samples is noticed owing to the presence of these defects and breakdown of attached functional groups. Thermal properties obtained from DSC, DMA, and TMA studies are presented in Table 2.

The effect of pristine or functionalized CNT on crystallization and melting behavior of PA6 was investigated using DSC. Figure 5(a) shows the crystallization behavior of neat polyamide and its composites containing 0.5 wt% P-CNT or N-CNT loading while cooling from 270°C to room temperature at 10°C/min. The presence of pristine or functionalized CNT in PA6 cause an increase in the crystallization temperature (T_C) from 163 to 193°C. This improvement in the value of T_C clearly indicates that CNT act as a nucleating agent for the PA6 matrix. Interestingly, the degree to which an increase in crystallization

Table 1. Sample identification and crystallite size corresponding to different crystallographic peaks as determined using Scherrer equation for neat and composites PA6 samples.

| Sample ID | CNT type | CNT (wt%) | Crystallite size (t_{hkl}) nm | |
|---------------|------------------|-----------|-----------------------------------|----------------|
| | | | t_{200} | $t_{002, 220}$ |
| PA6 | × | 0 | 2.2 | 2.5 |
| 0.5 P-CNT/PA6 | Pristine | 0.5 | 7.8 | 6.5 |
| 1.0 P-CNT/PA6 | Pristine | 1.0 | 3.4 | 4.2 |
| 0.5 C-CNT/PA6 | -COOH | 0.5 | 5.4 | 5.3 |
| 0.5 N-CNT/PA6 | -NH ₂ | 0.5 | 5.5 | 5.6 |

CNT: carbon nanotubes; PA6: polyamide-6; P: pristine; C: carboxylic; N: amine.

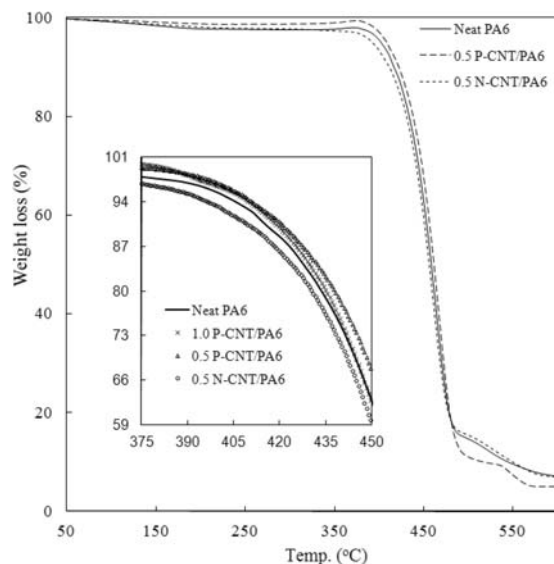


Figure 4. TGA thermograms of neat polyamide and different CNT/PA6 composites showing overall thermal behavior and comparison at the onset of thermal degradation (inset). CNT: carbon nanotubes; PA6: polyamide-6; TGA: thermogravimetric analysis.

temperature is observed, i.e. by $\sim 30^\circ\text{C}$, is the same regardless of surface of the nanotubes (unmodified or modified through functionalization treatment), indicating both similar level of affinity exhibited by PA6 to the nanotubes, and uniform, homogeneous dispersion of the nanotubes in the matrix for such loading. Although the value of T_C for neat PA6 samples, as determined during this study, is in the same range as reported in literature, it is strongly influenced by the cooling rate.⁴ Also, in contrast with earlier findings,^{20,21} a second crystallization peak was missing from the thermogram, presumably due to the relatively low loading level of the nanotubes. Figure 5(b) shows the melting behaviour of neat and composite PA6 samples upon heating to 270°C at a rate of $10^\circ\text{C}/\text{min}$. For all compositions, the melting peak appears at $\sim 220^\circ\text{C}$ with decrease in intensity upon CNT incorporation (pristine or functionalized) that is indicative of relatively less ordered packing or small size of the crystallites. The DSC data exhibited a single melting peak for all the samples, which is consistent with the findings of Liu et al.¹¹ Moreover, this single melting peak pertains to the presence of only α form crystal of PA6 upon inclusion of any CNT type. Furthermore, although there is a small exothermic peak present in the neat PA6 sample, the same peak is absent in the composites. The exothermic peak in neat PA6 depicts rearrangement of crystals or recrystallization during heating cycle of the DSC studies, however, due to the CNT nucleating effect, such exothermic peak does not appear in the CNT/PA6 composites.

Mechanical properties

The mechanical properties of the PA6 and P-CNT/PA6 composites were investigated using DMA. The graphical form of the tangent delta ($\tan \delta$, the ratio of loss modulus to the storage modulus, i.e. $\tan \delta = G''/G'$) versus temperature data, as shown in Figure 6(a), was utilized to determine glass transition temperature (T_g).

Table 2. Thermal and mechanical properties of neat and composites PA6 samples.

| Sample ID | Thermal properties | | | | Mechanical properties | | | |
|---------------|----------------------------|----------------------------|----------------------------|------------------------------|-----------------------|-----------|---------------------|------------------|
| | T_C ($^\circ\text{C}$) | T_m ($^\circ\text{C}$) | T_g ($^\circ\text{C}$) | CTE (ppm/ $^\circ\text{C}$) | E (GPa) | %E change | σ_{TS} (MPa) | ϵ_f (%) |
| PA6 | 162.5 | 220.8 | 62.5 | 0.435 | 1.66 | × | 39.3 | 34.0 |
| 0.5 P-CNT/PA6 | 192.6 | 219.3 | 63.5 | 0.413 | 2.05 | +23.5 | 55.2 | 5.5 |
| 1.0 P-CNT/PA6 | | | | 0.302 | 2.28 | +37.3 | 64.9 | 2.0 |
| 0.5 C-CNT/PA6 | | | | | 2.36 | +42.2 | 68.0 | 2.0 |
| 0.5 N-CNT/PA6 | 192.1 | 223.7 | 64.7 | | 2.66 | +60.2 | 69.1 | 1.5 |

CNT: carbon nanotubes; PA6: polyamide-6; P: pristine; C: carboxylic; N: amine; T_C : crystallization temperature; T_m : melting temperature; T_g : glass transition temperature; CTE: coefficient of thermal expansion; E: Elastic modulus; σ_{TS} : tensile strength; ϵ_f : strain at fracture.

The T_g value for neat PA6 is 62.5°C, which increases to 63.5 and 64.7°C, respectively, upon incorporation of pristine MWCNT with relatively low loading levels of 0.5 and 1.0 wt%. This trend is consistent with other

finding for CNT/PA6 composites.²² The incorporation and good dispersion of the nanotubes into the PA6 matrix enhances the degree of their mutual interaction, thus causing severe constraint on the motion of

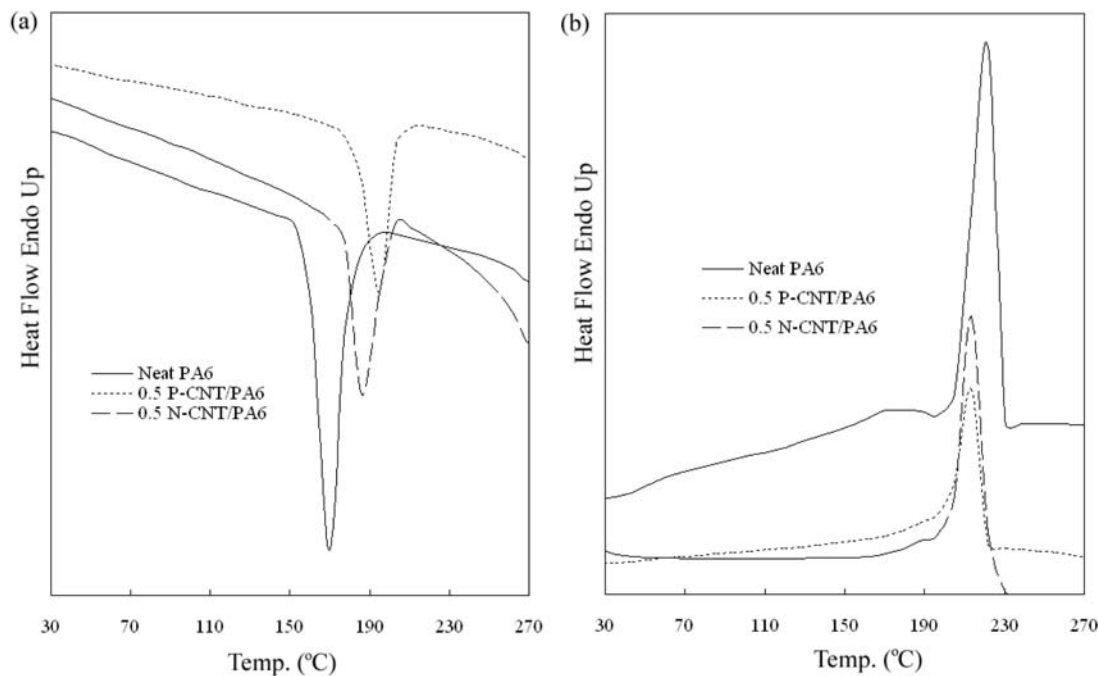


Figure 5. (a) DSC heating thermograms of neat and composite PA6 samples indicating onset of melting, and (b) DSC cooling curves showing crystallization behavior of PA6 composites with 0.5% P-CNT or N-CNT.

CNT: carbon nanotubes; DSC: differential scanning calorimeter; PA6: polyamide-6; TGA: thermogravimetric analysis.

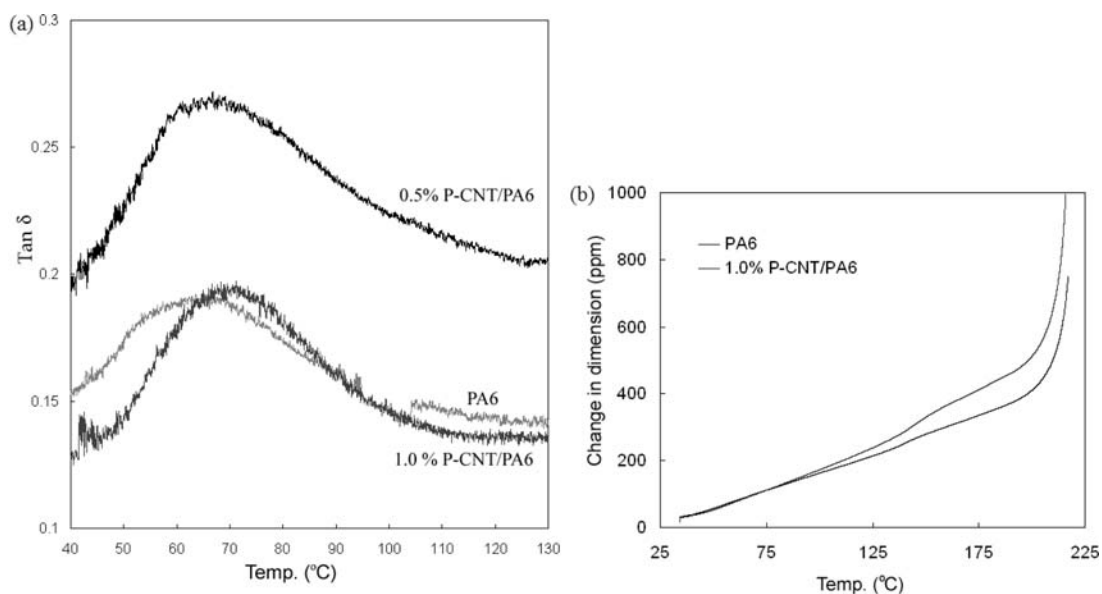


Figure 6. (a) $\tan \delta$ versus temperature for neat PA6 and P-CNT/PA6 composites and (b) change in dimension as a function of temperature as produced by thermomechanical analysis for computation of CTE values.

CNT: carbon nanotubes; PA6: polyamide-6.

polymer chains with an associated increase in the T_g value. Generally, an increase in T_g value also predicts improved elastic modulus and tensile strength levels in composites. The TMA studies led to estimation of coefficient of thermal expansion (CTE) using change in dimension as a function of temperature. The change in dimension versus temperature data for neat and composite polyamide samples is presented in Figure 6(b). From the slope of the linear segment, the value of CTE was computed. With increase in loading level of pristine CNTs, a decrease in CTE values was noticed. The findings confirmed resistance to relaxation imposed by uniformly dispersed nanotubes in the polymer matrix. With addition of only 1.0% P-CNT, the CTE value dropped significantly from 0.435 for neat PA6 to 0.302 ($10^{-6}/^{\circ}\text{C}$).

Results from tensile testing of the neat PA6 and composite specimens indicated increases in the values of modulus of elasticity (E) and tensile strength (σ_{TS}) upon MWCNT incorporation. Although addition of any type of MWCNT, whether pristine or functionalized, led to improvement in tensile properties, among all compositions, maximum degree of enhancement was observed in case of 0.5 N-CNT/PA6 specimens, where an improvement by ~ 61 and 76% was recorded in E and σ_{TS} values, respectively. The data obtained from tensile testing is graphically presented in Figure 7(a), whereas percent change in E and σ_{TS} values with respect to neat PA6 and strain to failure are listed in Table 2. The reported values for each composition were averaged from five trial runs and the standard deviation was found to be up to $\pm 3\%$ of the measured data. The

enhancement in E and σ_{TS} values can be attributed to efficient load transfer from the matrix to reinforcing nanotubes. Functionalization of nanotubes with either carboxylic or amine group is believed to improve dispersion into the polymer matrix as well as enhance load-bearing capacity of the composite, subsequently leading to higher stiffness and strength levels. The degree of change in mechanical properties is almost the same for 1.0 P-CNT/PA6 and 0.5 C-CNT/PA6 composites, indicating more effectiveness of carboxylic functionalized nanotubes with relatively less loading. The results obtained are in agreement with an earlier report on nylon 6 composites where an increase in tensile modulus by $\sim 87\%$ upon incorporation of amine-functionalized CNT was reported.⁹ There is an associated decrease in ductility as evident from drastic reduction in strain to failure upon CNT incorporation, as shown in graphical representation of data in Figure 7(b). Adding as little as 0.5 wt% of P-CNT causes a drastic decrease in strain at fracture to an average value of $\sim 5.5\%$. In case of functionalized nanotubes, this value further dropped to about 2% or less. It is speculated that whereas covalent functionalization of nanotubes leads to higher interfacial strength and subsequently efficient stress transfer mechanism, good CNT dispersion within the PA6 matrix also imposes extremely large constraint onto polymer chains due to reduced free volume of PA6. Nevertheless, the synthesis route adopted in this study indicated that melt compounding technique yields composites with similar or better mechanical attributes with much less nanotubes loadings as compared to those prepared using in-situ

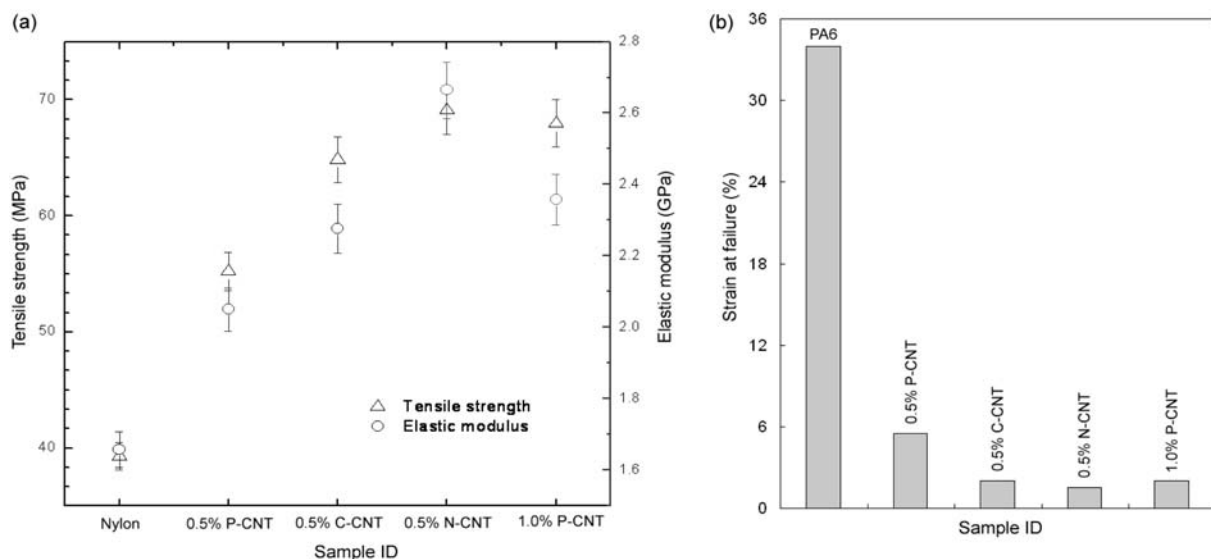


Figure 7. Mechanical properties of neat and composite PA6 specimens with different MWCNT types and loadings: (a) elastic modulus and tensile strength and (b) strain at failure. MWCNT: multi-walled carbon nanotubes; PA6: polyamide-6.

polymerization technique.⁴ Composites with amine-functionalized nanotubes exhibited better mechanical properties than those with carboxylic-functionalized CNT. Such behavior is due to more strong interfacial strength and greater bond length due to double-bond formation in case of N-CNT incorporation in contrast with C-CNT, which yielded weak single bond and relatively short bond lengths.^{23,24} The values of E , σ_{TS} , and strain at fracture as well as percent increase with respect to neat PA6 are listed in Table 2.

High-magnification surface microstructures of the neat and composite polyamide samples after cryofracture in liquid nitrogen are shown in Figure 8. The CNT incorporation appears to change the nature of fracture from predominantly ductile with high degree of roughness indicative of extensive plastic deformation (Figure 8(a)) to brittle with a relatively smooth surface as evident in case of PA6 composites reinforced with 0.5 wt% of P-CNT, C-CNT, or N-CNT (Figure 8(b)–(d)). The fractured surfaces of the composites revealed MWCNT presence with varying attributes. In case of 0.5 P-CNT/PA6 sample (Figure 8(b)),

the top central region shows a small cluster of few nanotubes protruding out suggesting less uniform dispersion inside matrix and relatively less interfacial strength compared with composites containing functionalized CNT. Upon functionalization with carboxylic acid group, dispersion characteristics were noticed to improve. Figure 8(c) shows 0.5 C-CNT/PA6 composite sample with several dots and segments of nanotubes up to $\sim 0.5 \mu\text{m}$ in length (indicated by arrows). During application of tensile load, the CNTs get stretched and eventually break leading to overall failure of the composite without undergoing extensive plastic deformation. In the absence of pull-out from matrix, such failure should appear as a dot, representing the point where nanotubes break. The presence of few nanotubes that seemed to have experienced debonding and pull-out from PA6 matrix during tensile testing, beside several dots indicative of CNT rupture, implies less efficient load transfer from the PA6 matrix to the C-CNT. Amine-functionalization treatment significantly improved CNT adhesion to PA6 through more intensive sidewalls modification and

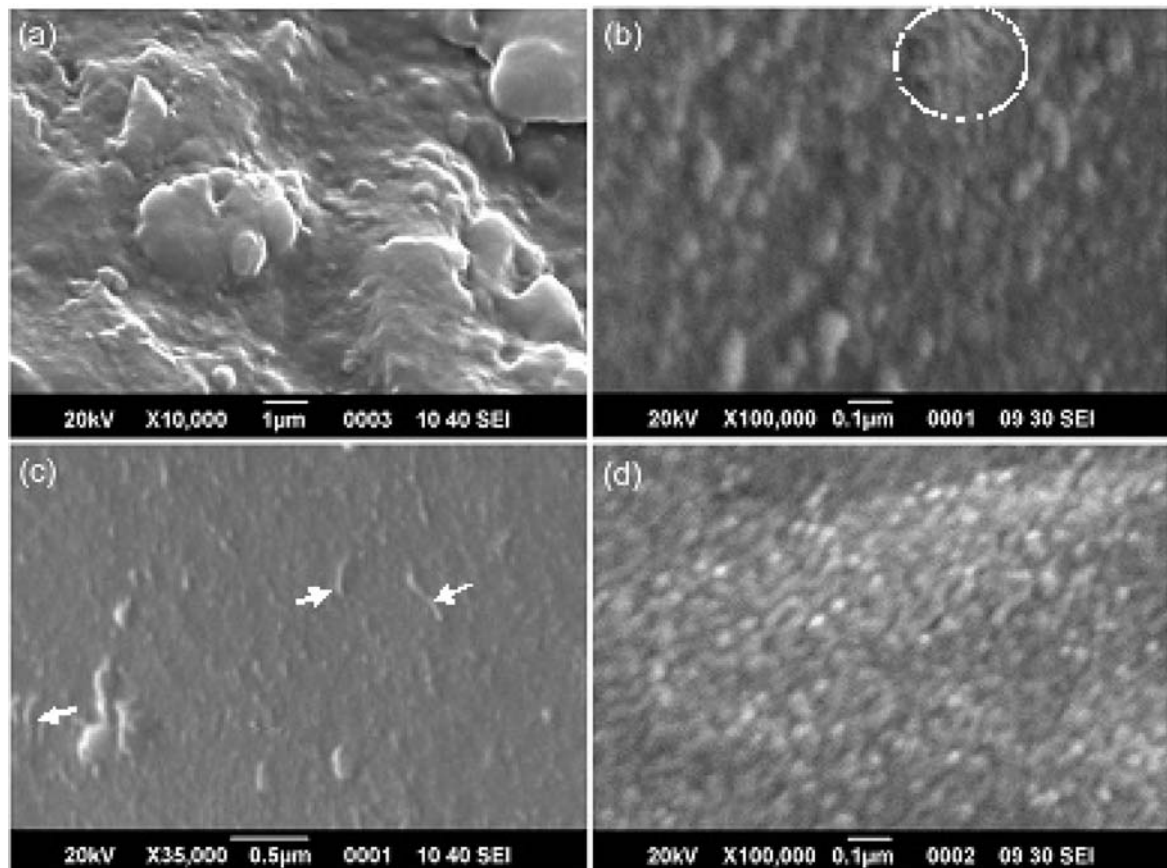


Figure 8. High-magnification SEM microstructures of the surfaces after cryofracture in liquid nitrogen: (a) Neat PA6, (b) 0.5 P-CNT/PA6, (c) 0.5 C-CNT/PA6, and (d) 0.5 N-CNT/PA6.

SEM: scanning electron microscope; CNT: carbon nanotubes; PA6: polyamide-6.

subsequently very efficient load transfer from the matrix to the CNT ensured formation of a dotted structure for N-CNT-reinforced composites, as shown in Figure 8(d). SEM studies of the fractured surfaces support a trend of increasing degree of improvement in tensile properties with associated decrease in strain to failure upon MWCNT incorporation with extensive surface functionalization. Thus, N-CNT-reinforced PA6 composites offer excellent dispersion characteristics and strong interfacial strength between the nanotubes and the PA6 matrix. Although pullout mechanism is dominant in strengthening of the PA6 matrix, sword-in-sheath mechanism (the MWCNT outermost shell remains attached to the polymer; the inner tube(s) fracture and are pulled out of this outer tube(s)) might also have a contribution assuming some degree of alignment between CNT was induced during melt extrusion.²⁵

Conclusions

Polyamide matrix was reinforced with different MWCNT types and 0.5 or 1.0 wt% loading using melt extrusion technique. HRTEM examination confirmed dissolution of catalyst nanoparticles and generation of defects on outermost surface of nanotubes as induced by chemical functionalization, whereas attachment of $-\text{COOH}$ and $-\text{NH}_2$ groups was indicated by signature peaks in the FTIR spectra. Addition of as low as 0.5 wt% MWCNT was found to enhance degree of crystallinity in the resulting composites through formation of more stable α -form crystals with nanotubes offering nucleation sites for PA6. There is also an associated increase in crystallite size upon CNT addition. SEM examination of cryogenically fractured surface pointed out to the formation of strong interface between nanotubes and the nylon-6 matrix and consequently effective load transfer from the matrix to the reinforcing CNT, as manifested by little or no evidence of nanotubes debonding from the matrix.

Thermogravimetric analysis revealed that thermal stability of composites containing 0.5 wt% P-CNT improved as compared to neat PA6, while those with 1 wt% P-CNT loading or functionalized nanotubes slightly decreased due to defects on sidewalls and attached functional groups. Addition of 0.5 wt% CNT increases the T_C value from ~ 162 to 192°C with slight increase in T_m values. DMA and TMA studies confirmed uniform dispersion of nanotubes within matrix leading to reduced free volume of the polymer caused by the restraining effect of nanotubes, as manifested by small increase in T_g values and a significant drop in CTE of the composites. For all composite compositions, the mechanical properties improved with a corresponding decrease in plasticity. The introduction

of amine-functionalized nanotubes with loading levels of 0.5 wt%, however, produced composites (0.5 N-CNT/PA6) with respective E and σ_{TS} values of 2.66 GPa and 69.1 MPa, an increase by ~ 60.2 and 75.8% when compared to neat PA6.

Among pristine (P), carboxylic- (C), and amine- (N) functionalized CNT, incorporation of 0.5 wt% P-CNT into PA6 matrix imparts higher degree of improvement in thermal properties through preferential nucleation and growth of stable α form crystals and increase in crystallite size. On the other hand, 0.5 N-CNT/PA6 composites show maximum increase in elastic modulus and tensile strength values owing to efficient load transfer from PA6 matrix to the CNT through uniform dispersion and strong interfacial bonding with the PA6 matrix.

Acknowledgements

The authors deeply appreciate financial support for this research from National University of Sciences and Technology, Islamabad, Pakistan. Also, technical assistance offered by Mr. Nicolas Gautier of Institut de Matériaux, Université de Nantes, France, in performing HRTEM studies is thankfully acknowledged.

Conflict of Interest

None declared.

References

1. Kiang CH, Endo M, Ajayan PM, et al. Size effects in carbon nanotubes. *Phys Rev Lett* 1998; 81(9): 1869–1872.
2. Lourie O and Wagner HD. Evaluation of Young's modulus of carbon nanotubes by micro-Raman spectroscopy. *J Mater Res* 1998; 13(9): 2418–2422.
3. Karapappas P, Vavouliotis A, Tsotra P, et al. Enhanced fracture properties of carbon reinforced composites by the addition of multi-wall carbon nanotubes. *J Compos Mater* 2009; 43(9): 977–985.
4. Zeng H, Gao C, Wang Y, et al. In situ polymerization approach to multiwalled carbon nanotubes-reinforced Nylon 1010 composites: Mechanical properties and crystallization behavior. *Polymer* 2006; 47: 113–122.
5. Ma PC, Siddiqui NA, Marom G, et al. Dispersion and functionalization of carbon nanotubes for polymer-based composites: A review. *Compos: Part A-Appl* 2010; 41: 1345–1367.
6. Zhang WD, Phang IY, Shen L, et al. Polymer composites using urchin-shaped CNT-silica hybrids as reinforcing fillers. *Macromol Rapid Commun* 2004; 25: 1860–1864.
7. Mahfuz H, Adnan A, Rangari VK, et al. Enhancement of strength and stiffness of nylon 6 filaments through carbon nanotubes reinforcement. *Appl Phys Lett* 2006; 88: 083119.
8. Gao J, Zhao B, Itkis ME, et al. Chemical engineering of the single-walled carbon nanotube–nylon 6 interface. *J Am Chem Soc* 2006; 128: 7492–7496.
9. Chen GX, Kim HS, Park BH, et al. Multi-walled carbon nanotubes reinforced nylon 6 composites. *Polymer* 2006; 47: 4760–4767.

10. Logakis E, Pandis C, Peoglos V, et al. Structure–property relationships in polyamide 6/multi-walled carbon nanotube composites. *J Polym Sci Part B* 2009; 47: 764–774.
11. Liu T, Phang IY, Shen L, et al. Morphology and mechanical properties of MWCNT reinforced nylon-6 composites. *Macromolecules* 2004; 37: 7214–7422.
12. Yu J, Tonpheng B, Gröbner G, et al. Thermal properties and transition studies of multi-wall carbon nanotube/nylon-6 composites. *Carbon* 2011; 49: 4858–4866.
13. Wang X, Bradford PD, Liu W, et al. Mechanical and electrical property improvement in CNT/nylon composites through drawing and stretching. *Compos Sci Technol* 2011; 71: 1677–1683.
14. Kakade BA and Pillai VK. An efficient route towards the covalent functionalization of single walled carbon nanotubes. *Appl Surf Sci* 2008; 254: 4936–4943.
15. Ma PC, Kim JK and Tang BZ. Functionalization of carbon nanotubes using a silane coupling agent. *Carbon* 2006; 44: 3232–3238.
16. Chang CM and Liu YL. Functionalization of multi-walled carbon nanotubes with furan and maleimide compounds through diels–alder cycloaddition. *Carbon* 2009; 47: 3041–3049.
17. Charles J, Ramkumaar GR, Azhagiri S, et al. FTIR and thermal studies on nylon-66 and 30% glass fibre reinforced nylon-66. *Europ J Chem* 2009; 6(1): 23–33.
18. Li L, Li CY, Ni C, et al. Structure and crystallization behavior of nylon 66/multi-walled carbon nanotube nanocomposites at low carbon nanotube contents. *Polymer* 2007; 48: 3452–3460.
19. Li J, Tong L, Fang Z, et al. Thermal degradation behavior of multi-walled carbon nanotubes/Polyamide 6 composites. *Polym Degrad Stab* 2006; 91: 2046–2052.
20. Saeed K and Park SY. Preparation of multiwalled carbon nanotube/nylon-6 composites by in situ polymerization. *J Appl Polym Sci* 2007; 106: 3729–3735.
21. Krause B, Pötschke P and Häußler L. Influence of small scale melt mixing conditions on electrical resistivity of carbon nanotube-polyamide composites. *Compos Sci Technol* 2009; 69: 1505–1515.
22. Logakis E, Pollatos E, Pandis C, et al. Structure–property relationships in isotactic polypropylene/multi-walled carbon nanotubes composites. *Compos Sci Technol* 2010; 70: 328–335.
23. Spitalsky Z, Tasis D, Papagelis K, et al. Carbon nanotube–polymer composites: chemistry, processing, mechanical and electrical properties. *Prog Polym Sci* 2010; 35: 357–401.
24. Gao C, Vo CD, Jin YZ, et al. Multihydroxy polymer-functionalized carbon nanotubes: synthesis, derivatization, and metal loading. *Macromolecules* 2005; 38: 8634–8648.
25. Blanco J, Garcia EJ, De Villoria RG, et al. Limiting mechanisms of mode I interlaminar toughening of composites reinforced with aligned carbon nanotubes. *J Compos Mater* 2009; 43(8): 825–841.